

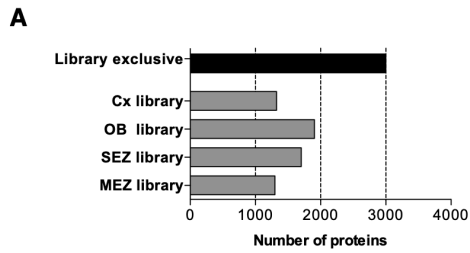
Cell Stem Cell, Volume 26

Supplemental Information

Defining the Adult Neural Stem Cell Niche Proteome

Identifies Key Regulators of Adult Neurogenesis

Jacob Kjell, Judith Fischer-Sternjak, Amelia J. Thompson, Christian Friess, Matthew J. Sticco, Favio Salinas, Jürgen Cox, David C. Martinelli, Jovica Ninkovic, Kristian Franze, Herbert B. Schiller, and Magdalena Götz



B

Protein Class	Number of proteins (of 2692)	Fold Enrichment	P-value
transcription factor	204	1.51	1.68E-06
Unclassified	1363	1.08	0.00E00
hydrolase	140	0.73	6.20E-03
RNA binding protein	88	0.65	1.54E-03
membrane traffic protein	40	0.52	5.40E-04
dehydrogenase	24	0.51	2.94E-02
ribosomal protein	18	0.41	1.60E-03

Protein
Dlx5
Dlx6
Foxj2
Foxp1
Foxp2
Pax6
Prox1
Rybpb
Smad1
Smad3
Sox2
Sox10
Sox11
Tbx21

C

Molecular Function	Number of proteins (of 2692)	Fold Enrichment	P-value
ubiquitin-protein ligase activity	47	1.80	2.20E-02
sequence-specific DNA binding transcription factor activity	162	1.58	2.74E-06
DNA binding	191	1.47	2.06E-05
receptor activity	114	1.40	4.66E-02
Unclassified	1356	1.06	0.00E00
catalytic activity	693	.87	9.28E-04
structural molecule activity	93	.67	3.05E-03
structural constituent of ribosome	16	.40	1.73E-03

Protein
CD47
Fzd5
Htra1a,b
Htra2a,c
Ifngr1
Ngfr
Ntsr1
Tgfbf1

D

Neurogenesis associated proteins

IL16	IL18	IL34
Igf1	Igf2	Igfbp6,7
Fzr1	Csf1	Pdgfra
Notch1	Notch2	Notch3
Rxra,g	Sirpa	Tgfb3
Uhrf1	Vegfa	Wnt4
Wnt5a	Wnt9a	

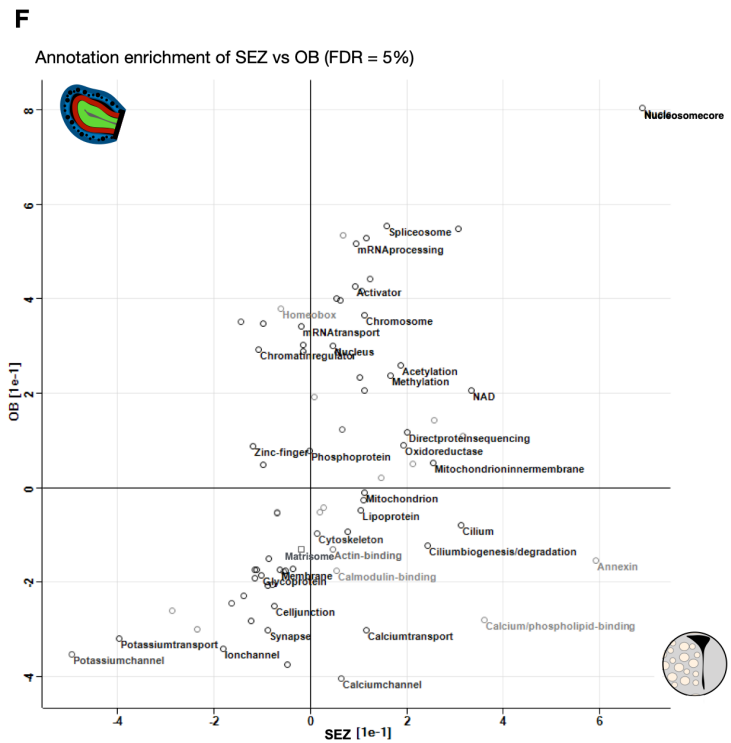
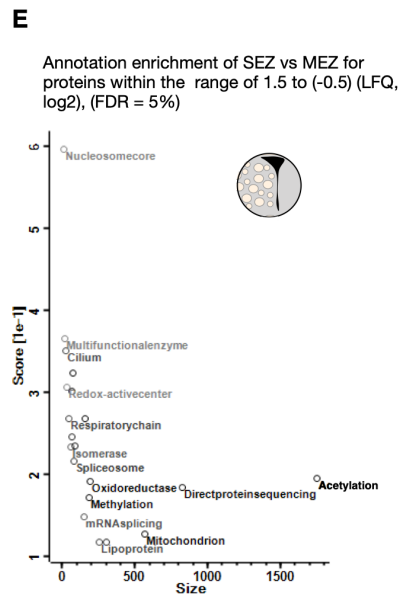


Figure S1, Related to Fig. 1H-M. Library-exclusive proteome is enriched in mitogens, cytokines, and transcription factors. The proteome depth achieved within the library measurements allowed greater detection of e.g. mitogens, cytokines, and transcription factors in vivo compared to single shot measurements. A) Number of proteins exclusive to the library measurements. B) Gene ontology of “protein class” with Panther (pantherdb.org) shows transcription factors significantly enriched among the library-exclusive proteins (red=positive enrichment, blue=negative enrichment) and C) gene ontology of “molecular function” shows receptor activity (e.g. growth factor receptors) significantly enriched among the library-exclusive proteins. D) Further examples of mitogens and cytokines exclusively detected in the library samples. E) The MEZ contains parts of the neurogenic niche (see discussion) and typically the neurogenic niche-associated proteins can be detected with lower LFQ intensities. Hence, we selected proteins with a similar abundance in SEZ and MEZ that had LFQ intensities within a range of 1.5 (log₂ fold) and -0,5 (log₂ fold) comparing SEZ to MEZ. This was used to bioinformatically remove potential non-neurogenic contamination. Subsequent enrichment analysis was performed as in Figure 1M. F) We compared the feature-enrichment of both OB and SEZ (input data was relative to Cx as in Figure 1L,M) and note that both enrich in nucleus and gene regulation (2D-annotation enrichment, FDR=0.05).

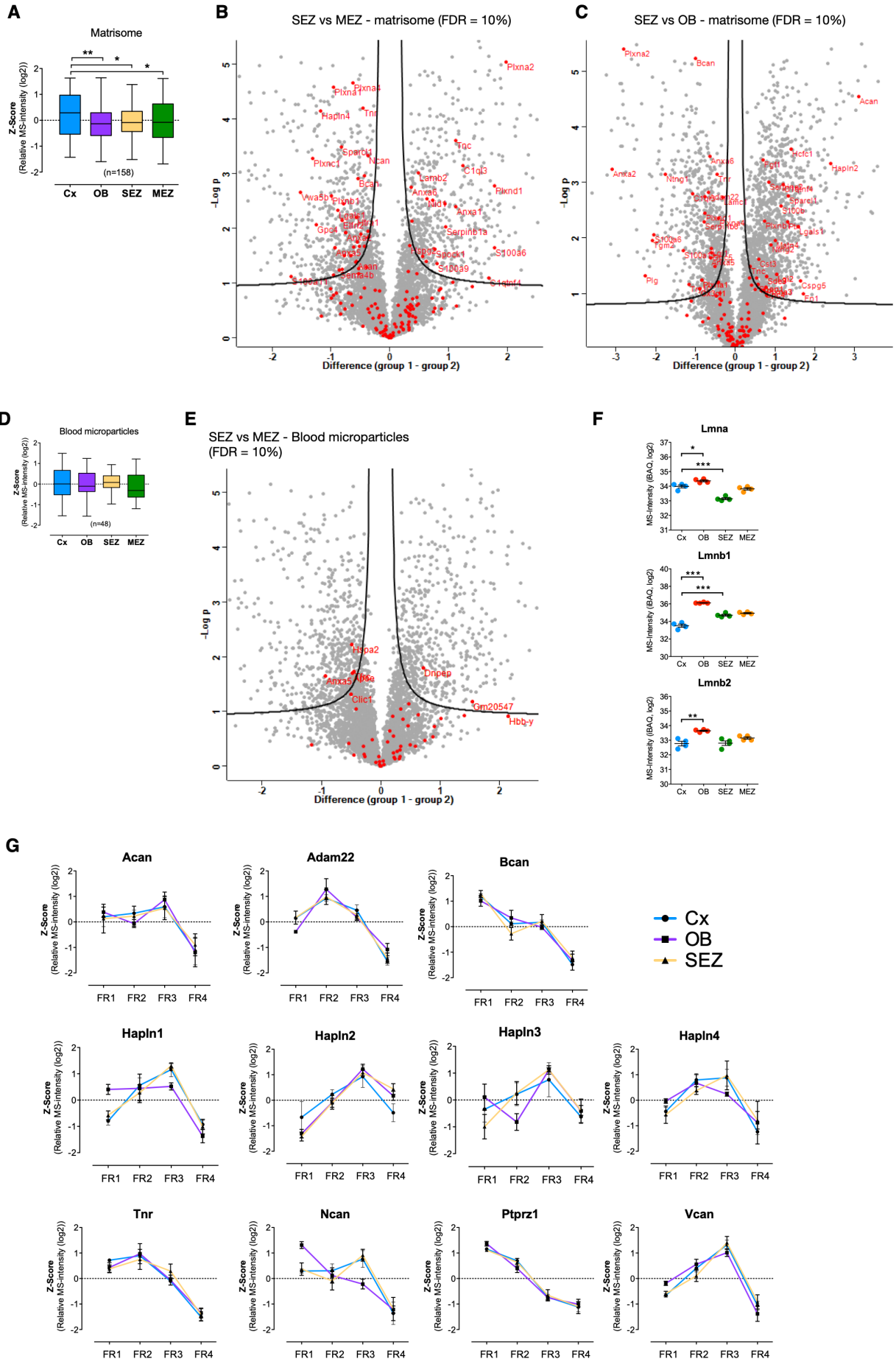


Figure S2, Related to Fig. 2. Niche matrisome, nuclear lamin, and perineuronal nets.

A) Distribution plots for the matrisome proteins of each brain region. Average LFQ intensities for each protein have been z-scored and are displayed in Whisker plots (ANOVA, Kruskal-Wallis test with Dunn's multiple comparison test, * $p=0.05$, ** $p=0.01$, and *** $p=0.001$). B) Volcano plots of SEZ and MEZ protein abundance values with matrisome proteins highlighted in red. Significance was analyzed using two-tailed t-test with FDR=0.1 ($S_0=0.1$). C) Abundance difference was analyzed in the same manner for SEZ and OB. D) Since the proteins of the blood microparticle category had similar abundance, blood proteins were not the reason for differences in regional matrisome distributions. Data shown as Whisker plots, ANOVA, * $p=0.05$, ** $p=0.01$, and *** $p=0.001$. E) Among the blood microparticle proteins, we find only a couple of significantly enriched proteins in the SEZ (and four in the MEZ) (two-tailed t-test, FDR=0.1, $S_0=0.1$). F) LFQ intensities of lamin-A, B1, and B2 from the LMSS experiment (ANOVA with Bonferroni's multiple comparison test, * $p=0.05$, ** $p=0.01$, and *** $p=0.001$). Data are presented as mean SEM. G) Each of the 11 proteins included in the PNN plot (Figure 2A) is shown here with individual solubility plots. Data is displayed as z-scored LFQ intensities of the four fractions of each protein and are presented as mean SEM.

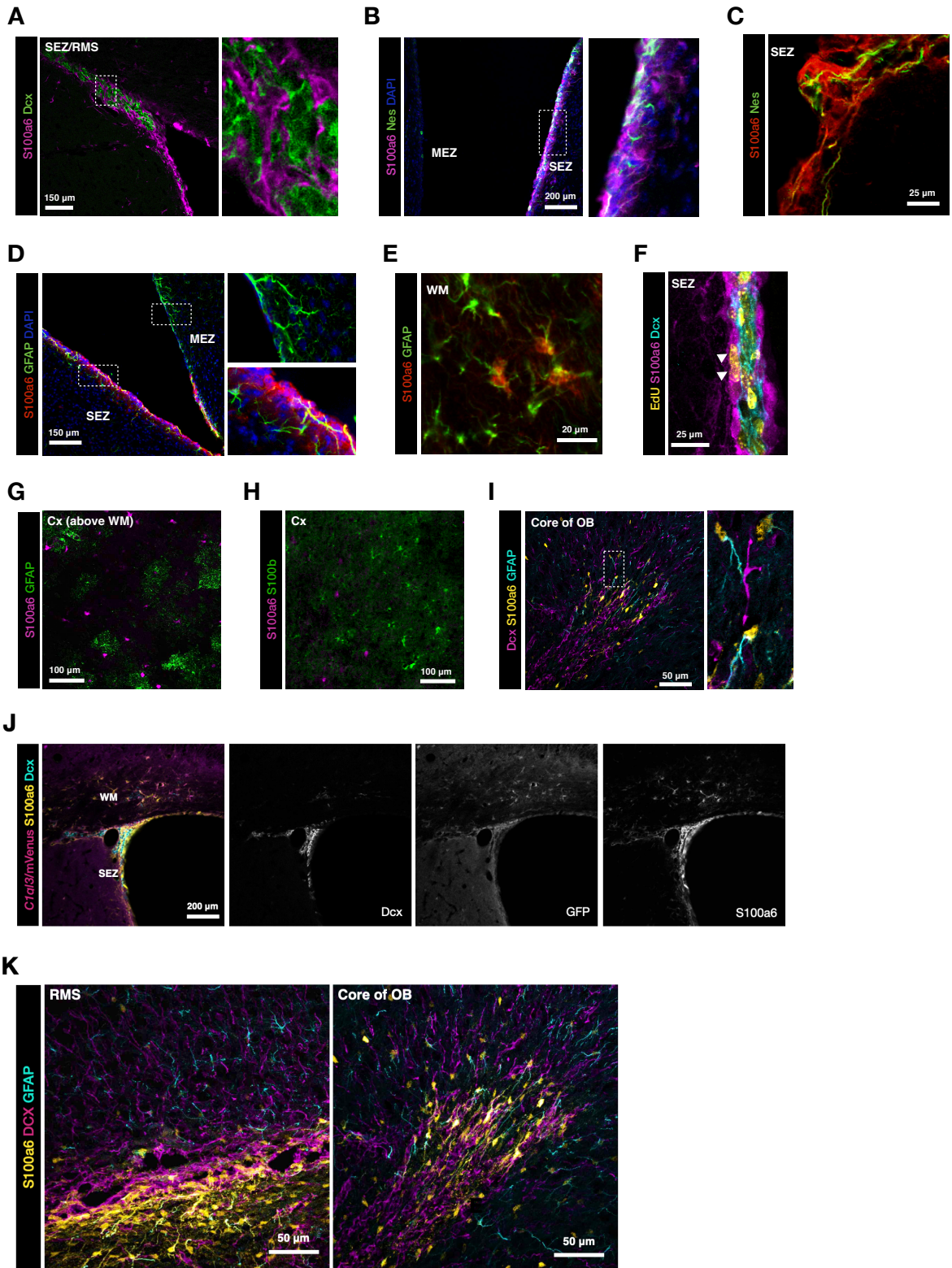


Figure S3, Related to Fig. 3. S100a6 in the neurogenic niches. A) Photomicrograph of immunostainings with S100a6 and Dcx highlight their proximity, but separate localization. B-C) S100a6 colocalizes with Nestin⁺ processes at the SEZ and D-E) colocalization with GFAP can be found at the SEZ (picture = confocal Z-stack) and in the white matter (WM, of corpus callosum). F) EdU was administered for 4 weeks and proliferation of S100a6⁺ cells was assessed. Note the EdU⁺/S100a6⁺ cells highlighted by arrowheads. G-H) S100a6 did not colocalize with GFAP nor S100b in Cx, instead, as shown in I) S100a6/GFAP colocalization could be found in the OB, in or in close proximity of the RMS. J) S100a6 and mVenus/C1q/3 (detected by GFP immunostaining) are colocalized in the WM consistent with the presence of some NSCs there, above the niche. K) Photomicrograph of immunostainings with S100a6, Dcx and GFAP in a sagittal section of the RMS/OB. As the neural stem cell niche ends, so do the majority of S100a6-high cells. S100a6-low cells (GFAP-positive cells) can be seen throughout the OB with somewhat higher density at the final length of the RMS in the OB (picture = stack composite). Scale bars as indicated in the panels. Figure S3D,J,K are Z-stacks of confocal pictures .

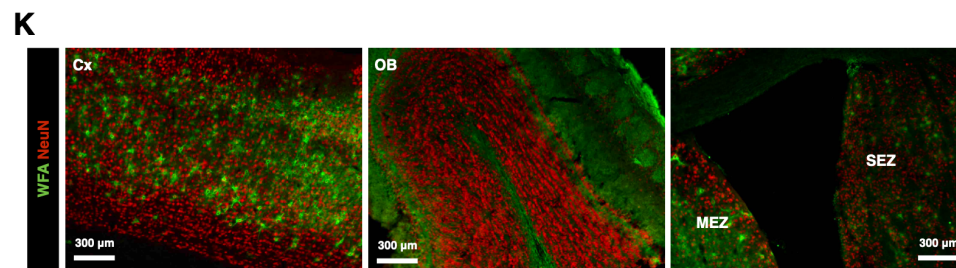
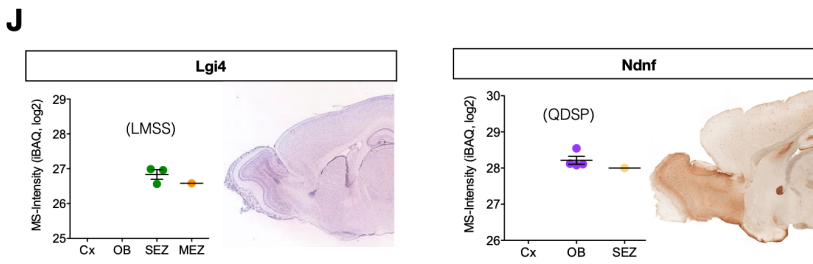
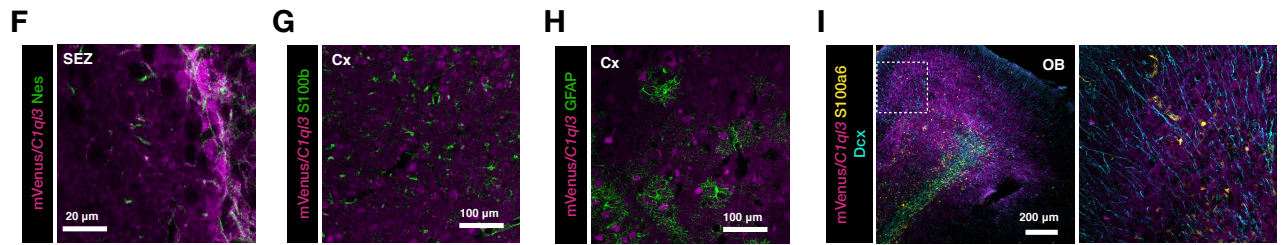
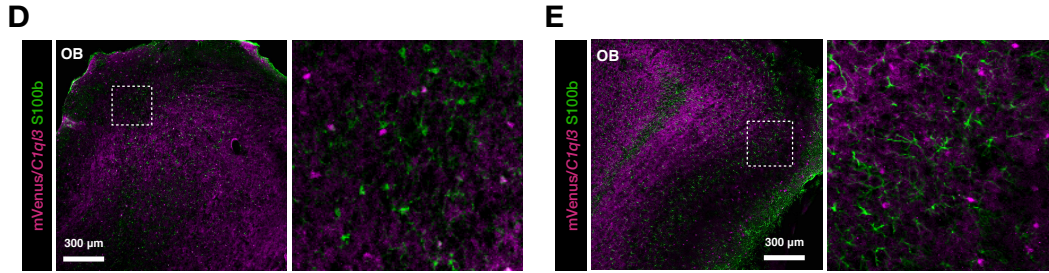
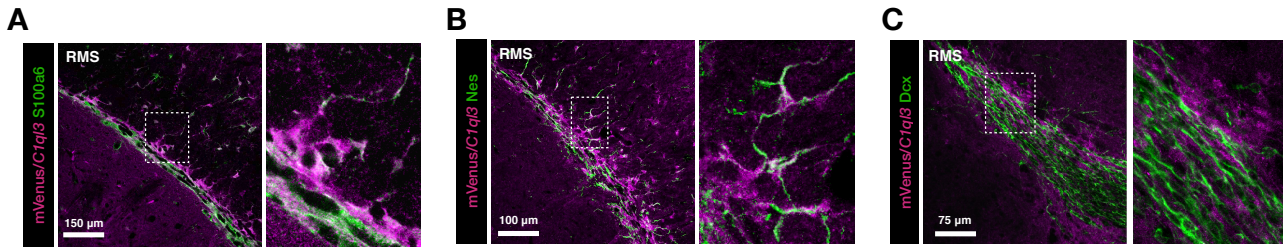


Figure S4, related to Figure 5. C1qI3, PNNs and additional new candidates at the neurogenic niches. At the beginning of the rostral migratory stream (RMS), we found mVenus/*C1qI3* to colocalize with S100a6 (A) and Nestin (B). C) mVenus/*C1qI3*⁺ cells surround the Dcx⁺ neuroblasts also in the middle of the RMS. D) mVenus/*C1qI3* was mostly diffuse in the OB, but also labeled some GFAP⁻ and E) S100b⁻ cells. F) Nestin⁺ processes in the SEZ are often mVenus/*C1qI3* positive. G-H) In the Cx, mVenus/*C1qI3* does not colocalize with either GFAP, nor S100b. I) Contrary to the SEZ, in the OB mVenus/*C1qI3* does not colocalize with S100a6. Image is a confocal Z-stack. J) Matrisome proteins Leucine Rich Repeat LGI Family Member 4 (*Lgi4*) and Neuron Derived Neurotrophic Factor (*NDNF*) were only quantified in the LMSS data and the QDSP data, respectively. Data are presented as mean ± SEM. *Lgi4* seems enriched at the SEZ and *NDNF* seems enriched in the OB. *Lgi4* in situ-hybridization originates from Allen brain atlas. Image credit: Allen institute for Brain Science. *Ndnf* expression (EGFP) pictures originate from GENSAT gene expression atlas. Image credit: GENSAT project at Rockefeller. K) Perineuronal nets were stained using the lectin *Wisteria floribunda* (WFA) that binds N-acetylgalactosamine on carbohydrates. Perineuronal nets were identified in the Cx when immunostained with WFA and NeuN to label neurons (left panel), while none are stained in the OB (middle panel) and SEZ (right panel). Scale bars as indicated in the panels.

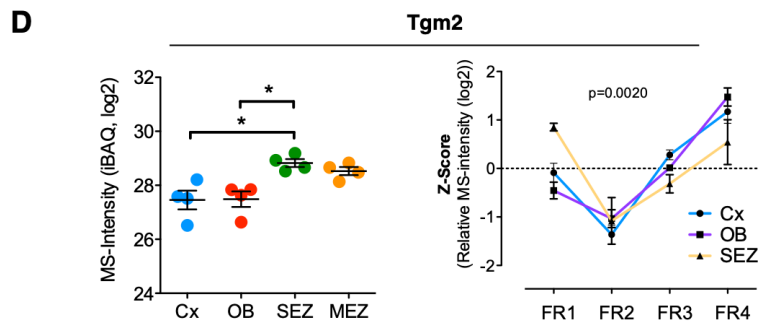
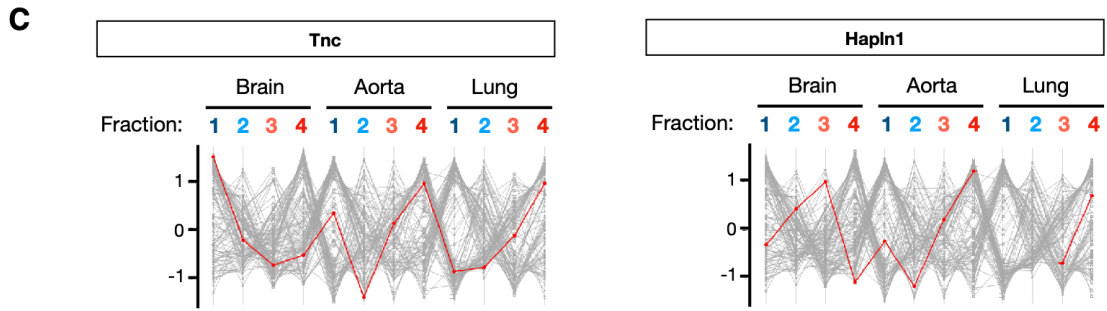
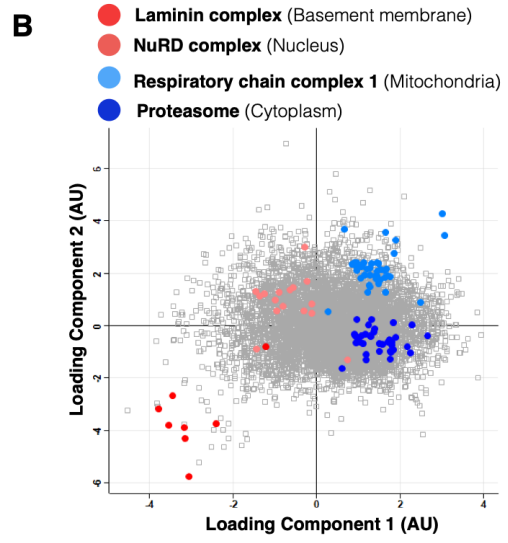
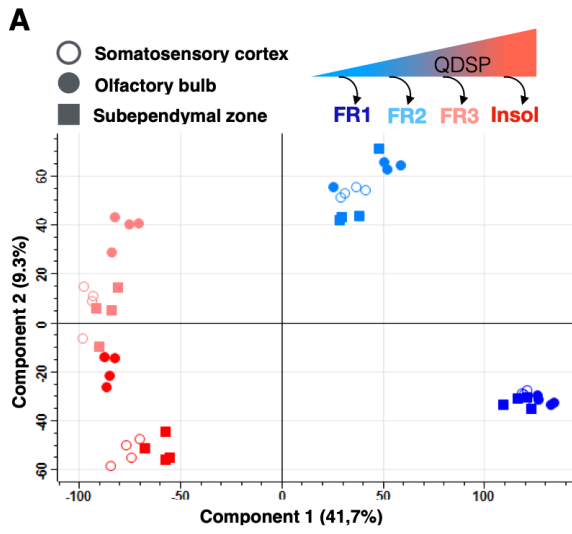
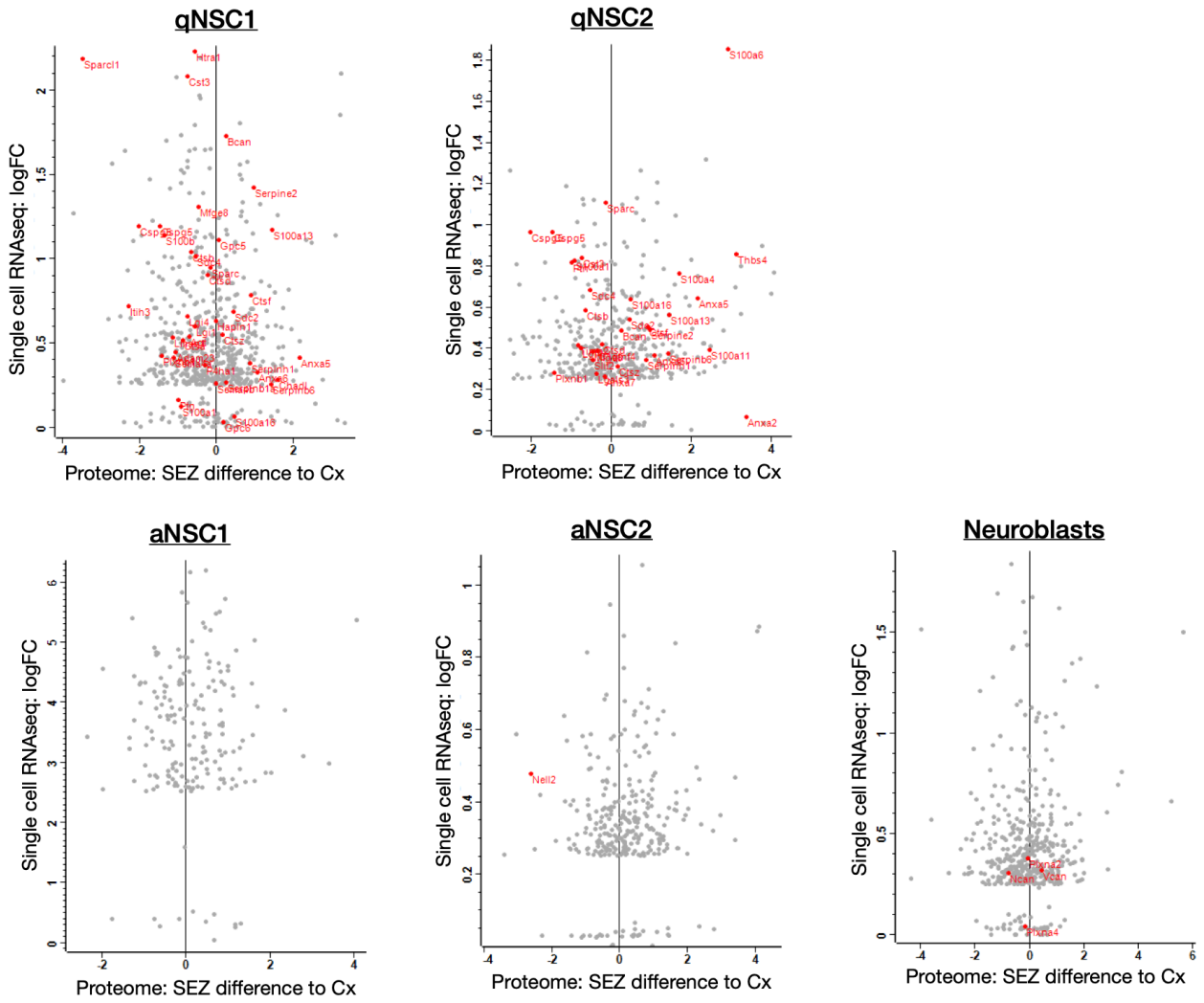


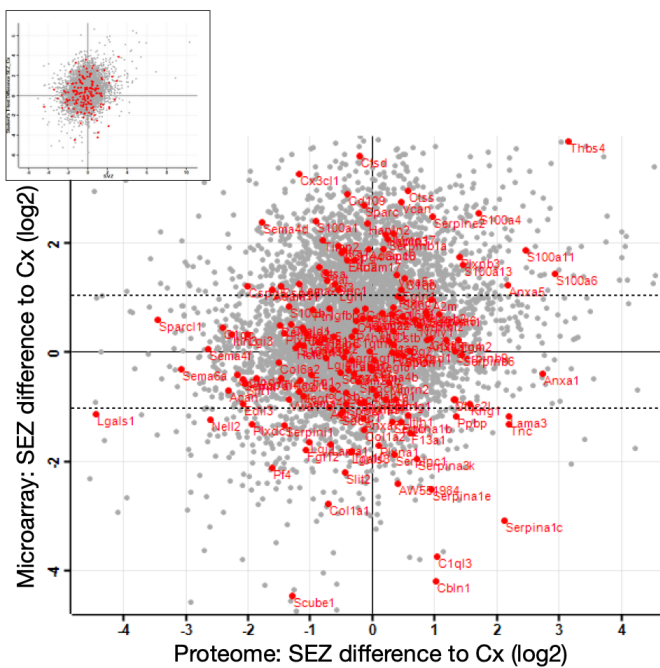
Figure S5, Related to Fig. 6. QDSP comparisons and Transglutaminase 2 measurements. A) Principal component analysis (PCA) for each brain region and detergent fraction. Component 1 and 2 separates the detergent fractions. B) In the scatterplot (of the PCA), we display four categories (in color) with significant enrichment for each of the four fractions ($FDR \leq 0.05$). C) We compared the brain matrixome data to previously published data sets using the QDSP method in aorta and lung tissue (Schiller et al. 2015, Wierer et al. 2018). Overall, many proteins have a similar profile in the different tissues, but some ECM proteins such as for example Tnc and Hapln1 have drastically different solubility profiles (more soluble in brain). The averaged data sets here are comprised of an average from all experimental groups of each study. D) Tgm2 proteome data from the LMSS data-set (left plot) (ANOVA with Bonferroni's multiple comparison test, * $p=0.05$) and the QDSP data-set (right plot) (z-scored, 2way-ANOVA). In the QDSP data-set both Cx and OB contain meninges (only perenchyma in the LMSS dataset). This may be a reason for difference in solubility between the OB/Cx and the SEZ, since Tgm2 can be found in the meninges. Data are presented as mean SEM.

A

SEZ proteome comparison to the “Kalamakis et al. 2019” cell-specific RNA enrichment data from SEZ

**B**

SEZ proteome and microarray data relative to Cx data

**C**

OB proteome and microarray data relative to Cx data

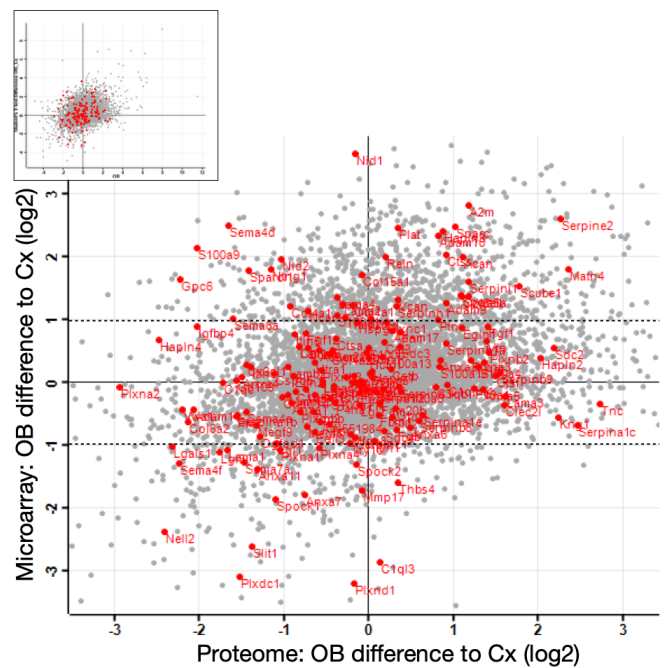
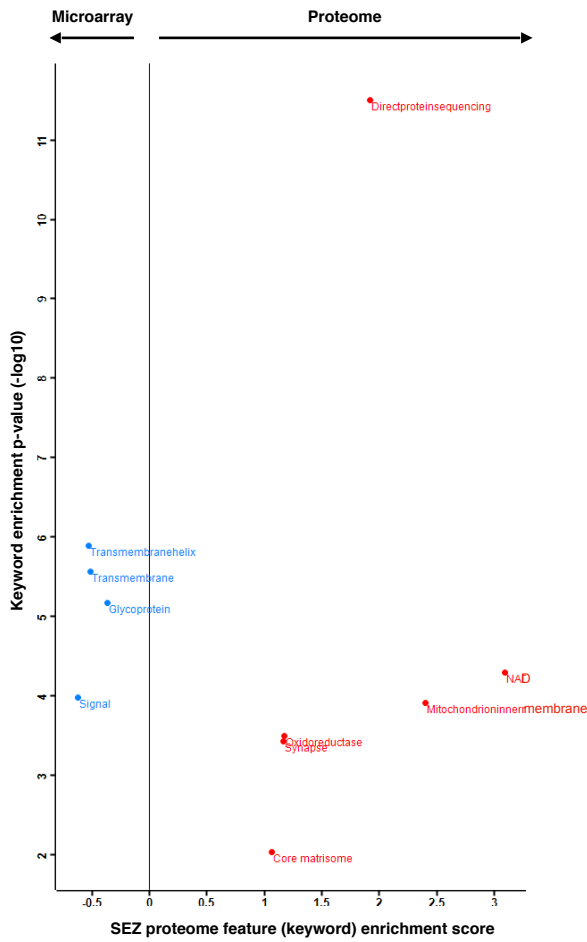


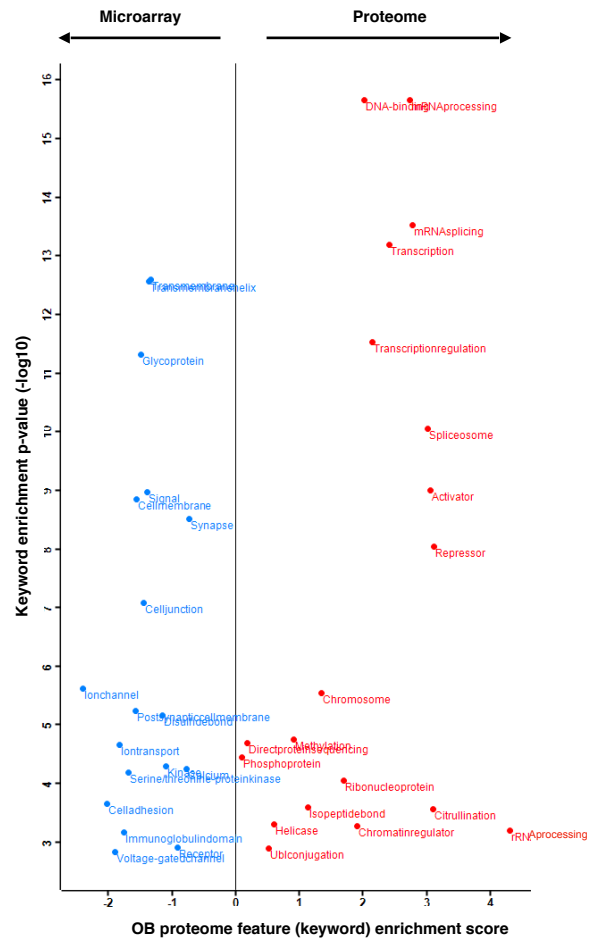
Figure S6, Related to Fig. 4. Comparison of the niche matrisome data with microarray and scRNAseq data. A) Kalamakis et al. (2019) used scRNAseq to analyse the neurogenic niche cells of the SEZ and determined cell-specific enrichment of the stem cell stage/subtype genes. The relative enrichment values from the scRNAseq was compared to the SEZ abundance normalized to Cx. Note that the niche-specific matrisome is abundantly expressed by quiescent neural stem cells (qNSCs), primarily the 2nd stage/subtype of the qNSCs. B-C) The microarray data originates from the same tissues as the proteome data (Cx, OB, and SEZ) and the data presented here had a cut-off of 2-fold difference to Cx. Both SEZ (B) and OB (C) was normalized to the Cx measurements from the respective data-sets and the relative matrisome abundance was compared as seen in the scatterplots (red = matrisome proteins/genes, grey = all proteins/genes). Significant regulation in the microarray data is defined by its p-value, and also as the fold change. The dashed line at 1 and -1 log₂ fold change highlights the minimum fold change for significant difference between SEZ and Cx. Note that while e.g. *Thbs4* in the SEZ correlates well between the proteome and microarray data, e.g. *C1ql3* was instead anti-correlated.

A

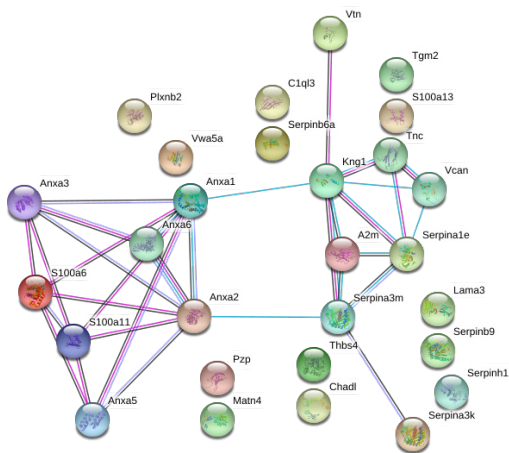
Relative enrichment of SEZ features in the proteome vs microarray data-set

**B**

Relative enrichment of OB features in the proteome vs microarray data-set

**C**

SVZ-enriched matrisome proteins in comparison to Cx (p-value cut-off = 0.1)

**D**

OB-enriched matrisome proteins in comparison to Cx (p-value cut-off = 0.1)

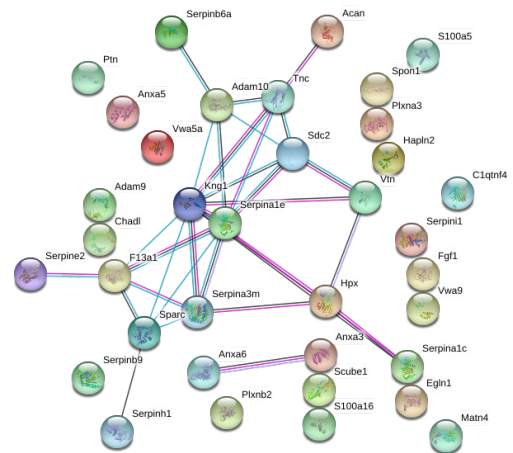


Figure S7, Related to Figure 4. Divergent -omics data features and niche-specific matrixome interactomes. A-B) The microarray data and proteome data in Fig. S6B,C was analysed for enriched features (2D-annotation enrichment, FDR=0.05, using the Uniport keyword annotation). The significantly enriched features are displayed with a relative score for the comparable enrichment in the proteome to the microarray in the SVZ (A) and the OB (B). (C-D) Enriched matrixome proteins ($p \leq 0.1$) of the SEZ in comparison to Cx (C) and OB in comparison to Cx (D) were analyzed in the STRING database (string-db.org) for known protein interactions.